2004), *Neurospora* (Nolan et al. 2005), and mice (Aravin et al. 2007; Carmell et al. 2007). Small RNAs against transposon sequences have been cloned in germlines, and the loss of Piwi family gene expression causes down-regulation of these small RNAs in *Drosophila*, zebrafish, and mice (Saito et al. 2006; Aravin et al. 2007; Brennecke et al. 2007; Gunawardane et al. 2007; Houwing et al. 2007). Based on these results, it has been suggested that the murine Piwi family genes are involved in retrotransposon gene silencing via small RNAs, probably repeat-associated piRNAs.

Retrotransposons are thought to be maintained in a transcriptionally silent state by DNA methylation (Walsh et al. 1998). During spermatogenesis, the DNA methylation status of the regulatory regions in retrotransposons, such as IAP (intracisternal A particle) and Line-1 (long interspersed nuclear elements), which belong to the long terminal repeat (LTR) and non-LTR retrotransposon families, respectively, changes dynamically (Tanaka et al. 2000; Lane et al. 2003). These regions are demethylated in PGCs around E12.5–E13.5, and the reacquisition of DNA methylation (i.e., de novo methylation) takes place in nondividing prospermatogonia (i.e., gonocytes) in the fetal testis around E16.5–E18.5. This de novo methylation involves either of the two de novo DNA methyltransferases, Dnmt3a and Dnmt3b, as well as their activating factor Dnmt3L, and analyses of Dnmt3L-deficient mice clearly show that this molecule is essential for the process (Bourc'his and Bestor 2004; Hata et al. 2006; Kato et al. 2007). Recently, it was reported that *Mili*- and *Miwi2*-targeted mice exhibited enhanced IAP and Line-1 expression, and methylation of the 5′-untranslated region (UTR) region of Line-1 was shown to be reduced in these mice at the neonatal stage (Aravin et al. 2007; Carmell et al. 2007). However, the DNA methylation status and piRNA expression of retrotransposons during de novo DNA methylation have not been examined. Thus, in the present study, we analyzed the piRNA expression and DNA methylation profiles of the IAP and Line-1 retrotransposons in fetal MILI-null and MIWI2-null testes.

Results

Comparison of Line-1 and IAP gene expression in MILI$^{-/-}$ and MIWI2$^{-/-}$ testes

To understand the roles of the mouse PIWI family proteins, we generated and analyzed MILI- (Aravin et al. 2007; Carmell et al. 2007) and MIWI2-deficient mice (Supplemental Fig. S1). In MILI- and MIWI2-null testes, spermatogenesis was arrested at the early prophase of meiosis I (Supplemental Fig. S1E). Affymetrix GeneChip microarray hybridization showed that five genes were up-regulated more than threefold in the *MILI*$^{-/-}$ testes, and all of these genes belonged to the IAP retrotransposon (Supplemental Fig. S2). The Line-1 and IAP gene expression levels were subsequently examined in the testes of 2-wk-old mice—i.e., testes that contained both premeiotic and meiotic germ cells—by Northern blotting (Fig. 1C,D). The transcripts of two representative Line-1 species, type Gf and type A, which have similar and unique sequences in their coding and 5′-noncoding regions, respectively, were similarly accumulated in both the MILI- and MIWI2-deficient testes. Meanwhile, expression of IAP was strongly and only slightly enhanced in the MILI- and MIWI2-null testes, respectively. Although the mouse genome contains full-length (7.2-kb) IAP elements and variants with deletions of various sizes in the *gag-pol* area (Ishihara et al. 2004), only the 5.4-kb IΔ1-type IAP transcript was enhanced in both mutants.

Reduced CpG methylation of Line-1 and IΔ1-type IAP in MILI$^{-/-}$ and MIWI2$^{-/-}$ germ cells

We examined the methylation status of the regulatory regions of Line-1 and IAP in MILI- and MIWI2-deficient male germ cells sorted 8–12 d after birth; namely, premeiotic germ cells. The promoter regions of type Gf and type A Line-1 in the sorted male germ cells were examined by bisulfite sequencing. As shown in Figure 1E, a significant reduction in CpG methylation was observed in the MILI- and MIWI2-deficient male germ cells at this stage. The reduction in methylation of type Gf Line-1 was confirmed by methylation-sensitive Southern blotting (Supplemental Fig. S3). Next, we analyzed the methylation pattern of CpG in two arbitrarily chosen LTR regions of the 5.4-kb IΔ1-type IAP on chromosomes 3 and 16. These regions were almost completely methylated in the control germ cells, whereas the levels of methylation were much lower in the MILI- and MIWI2-deficient germ cells (Fig. 1F).

Dnmt3L is essential for the de novo methylation of retrotransposons in fetal testes, and the testicular phenotype of Dnmt3L-null mice is essentially the same as those of MILI- and MIWI2-null mice (Bourc'his and Bestor 2004; Webster et al. 2005; Hata et al. 2006). Thus, we examined the DNA methylation status of the Line-1 regulatory regions in MILI- and MIWI2-deficient neonatal testes, which contain premeiotic germ cells. Methylation-sensitive Southern blot analysis revealed that hypomethylation was already present on day 2 after birth (Fig. 2A), as was seen in Dnmt3L-mutant mice. Bisulfite sequencing confirmed the impaired CpG methylation status of the Line-1 and IΔ1-type IAP regulatory regions in MILI- and MIWI2-deficient germ cells on day 0–1 after birth (Fig. 2B). It seems unlikely that the defective methylation in the MILI-deficient mice was due to decreased expression of Dnmt3L and/or its presumptive cooperating DNA methyltransferase, Dnmt3a2, since the expression of these methylases was unaffected by the mutation in *MILI* (Supplemental Fig. S4).

It is possible that MILI and MIWI2, as well as Dnmt3L, have roles in de novo methylation during male germ cell differentiation. Therefore, we carried out bisulfite sequencing of the regulatory regions of the Line-1 and IAP retrotransposons in MILI-deficient fetal germ cells around de novo methylation. In control germ cells, almost all of the CpGs in the LTRs of IAP were methylated soon after birth (Figs. 1F, 2B), whereas only incomplete

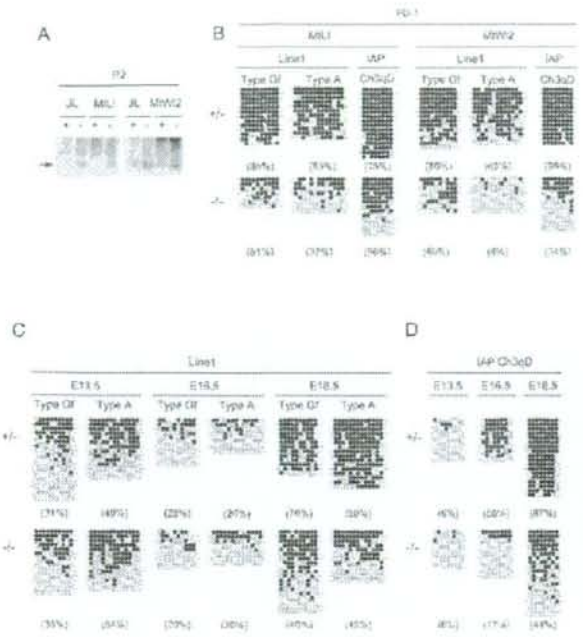

Figure 2. Methylation of the IAP and Line-1 regulatory regions in fetal testes. (*A*) Methylation-sensitive Southern blot analysis of the Line-1 promoter region. Whole-testis DNA was extracted from 2-d-old heterozygous (+) and homozygous (−) mice, followed by digestion with KpnI and the methylation-sensitive restriction enzyme HpaII. The probe for the type Gf Line-1 5′-noncoding region is the same as that in Figure 1C. (*B*) Bisulfite analysis of the Line-1 regulatory region in day 0–1 germ cells from MILI- and MIWI2-deficient and control testes. The germ cells were collected as described in Materials and Methods. (*C*,*D*) Bisulfite sequencing of the Line-1 (*C*) and IAP (*D*) regulatory regions in germ cells from MILI-deficient and control testes between E13.5 and E18.5. The germ cells were collected as described in Materials and Methods.

methylation was observed in E13.5, E16.5, and E18.5 germ cells (Fig. 2D). De novo methylation of the Line-1 and IAP regulatory regions of control mice occurred after E16.5 and E13.5, respectively (Fig. 2C,D). De novo methylation of Line-1 genes was slightly delayed compared with that of the IAP genes. In the MILI-deficient germ cells, hypomethylation of Line1 and IAP was observed at E18.5 and after E16.5, respectively. Differences in the methylation status of Line-1 in the MILI-deficient mice became apparent somewhat later than that of IAP, which seemingly reflects the delay of de novo methylation in the control germ cells. Our observations indicate that MILI plays an essential role in the timing of de novo methylation of the Line-1 and IAP regulatory regions.

Characterization of small RNAs in fetal testes

As discussed above, MILI and MIWI2 presumably function in gene silencing through DNA methylation in fetal testes. Based on the role of small RNAs from other organisms in gene silencing (Zaratiegui et al. 2007), it is possible that DNA methylation is mediated by small RNAs. Therefore, we analyzed many small RNA sequences (127,997 clones), 17–40 nt in length, from E12.5–E19.5 fetal male germ cells, to obtain a comprehensive picture of the piRNAs present at this stage, and compared our findings with the results of previous studies on piRNAs in neonatal (prepachytene) testes (Aravin et al. 2007) and adult testes (Aravin et al. 2006; Girard et al. 2006; Grivna et al. 2006; Lau et al. 2006; Watanabe et al. 2006). The lengths of the small RNAs from the germ cells showed a bimodal pattern (Fig. 3A). One peak was observed at ~21 nt, which corresponds to the lengths of miRNAs, and a second was observed at 25–27 nt, which is consistent with the lengths of piRNAs.

Annotation of the small RNAs revealed that the library was enriched with retrotransposon sequences, with the exception of the breakdown products of rRNAs and other noncoding RNAs (tRNA/snRNA/snoRNA/scRNA/srpRNA) (Fig. 3B; Supplemental Table S1). The repeat-associated small RNAs (rasiRNAs) in the library, which reportedly bind MILI, showed a single peak at 25–27 nt (Fig. 3A). The relative abundance of repeat-associated RNAs (23%) was similar to that of the MILI-associated prepachytene piRNAs identified in neonatal testis (26%) (Fig. 3B; Supplemental Table S1; Aravin et al. 2007). However, detailed characterization of the repeat-derived small RNAs revealed that there were some differences between the fetal germ cell piRNAs and the reported prepachytene piRNAs (Aravin et al. 2007). As shown in Supplemental Table S2 and Figure 3C, the majority of the rasiRNAs in the E16.5 male germ cells were LTR retrotransposons (55%); namely, ERVK (37%), ERV1 (10%), MaLR (6%), and ERVL (2%). The others were LINEs (30%) and SINEs (11%). In contrast, among the prepachytene piRNAs, the SINE frequency (49%) was higher than the LTR (33.8%) or LINE (15.8%) (Aravin et al. 2007) frequency. Unique pachytene piRNAs were scarcely detected in the fetal male germ cells (0.1%)

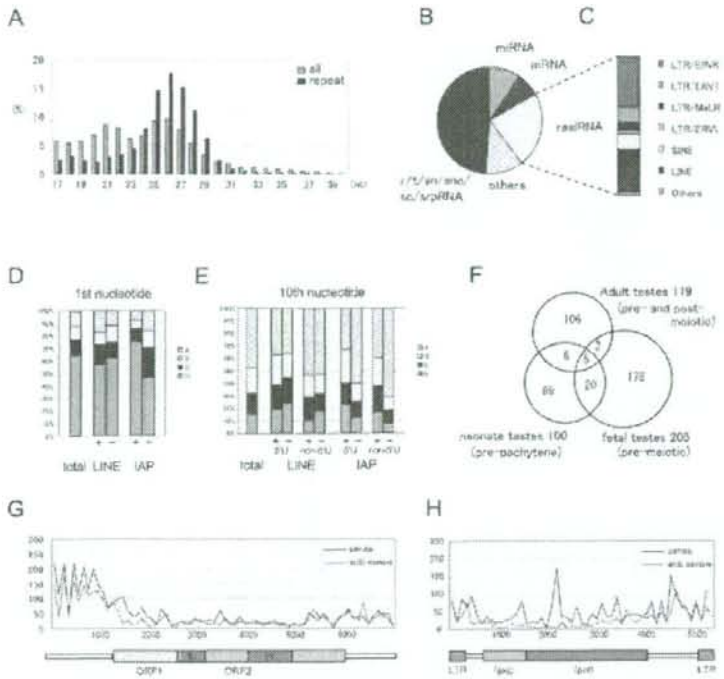

Figure 3. piRNAs in fetal premeiotic germ cells. (*A*) In total, 127,997 small RNAs were sequenced from E12.5–E19.5 fetal germ cells. The size distributions (in nucleotides) of the total small RNAs and rasiRNAs are shown by blue and purple bars, respectively. (*B*,*C*) Genomic annotation of the small RNAs (*B*) and the ratio of piRNA sequences of fetal premeiotic germ cells (*C*). Detailed results are listed in Supplemental Table S2. (*D*,*E*) Comparison of the first (*D*) and tenth (*E*) nucleotides of the total, sense (+), and antisense (−) piRNAs. Nucleotide biases were calculated for the Gf type Line-1 and IAP piRNAs analyzed in Supplemental Table S2. (*E*) The piRNA classes that contain or lack a 5′-end U are shown separately. (*F*) Venn diagram of the piRNAs in adult pre- and post-meiotic (Aravin et al. 2006; Girard et al. 2006; Grivna et al. 2006; Lau et al. 2006; Watanabe et al. 2006), neonatal prepachytene (Aravin et al. 2007), and fetal (this study) testes. (*G*,*H*) Distribution of piRNAs corresponding to type Gf Line-1 (*G*) and IAPIΔ1 (*H*).

(Supplemental Table S1). Next, as the small RNAs that correspond to Line-1 and IAP were abundant, we examined the nucleotide composition of the piRNAs corresponding to type Gf Line-1 and IAP retrotransposons. The first and tenth nucleotides of the piRNAs are shown in Figure 3, D and E. Most of the piRNAs started with uridine and had an adenine at the tenth position, which is similar to the characteristics of prepachytene piRNAs (Aravin et al. 2007).

Adult and neonatal piRNAs are clustered within the genome (Aravin et al. 2006, 2007; Girard et al. 2006; Grivna et al. 2006; Lau et al. 2006; Watanabe et al. 2006). Therefore, we performed a cluster analysis of the male fetal gonadal small RNAs and detected 205 clusters (Supplemental Table S3), only seven and 25 of which were identified in adult and prepachytene testes, respectively (Fig. 3F). About 75% of the clustered small RNAs were 24–28 nt in length, and the percentage of small RNAs with U as the first nucleotide was high (71.5%). Therefore, we conclude that most of the clusters are piRNA clusters, and that the set of piRNAs expressed at the stage of de novo methylation is quite different from the piRNA sets expressed in the neonate and adult.

The distribution and frequency plots of the piRNAs that correspond to the type Gf Line-1 and IAPIΔ1 genes are shown in Figure 3, G and H, respectively. For Line-1, the number of piRNAs that corresponded to the regulatory region was higher than that corresponding to the coding region, and the distributions of sense and antisense piRNAs were indistinguishable. Meanwhile, for the IAPIΔ1 genes, the number of sense piRNAs was slightly higher than the number of antisense piRNAs, and there were many piRNAs that corresponded to the coding region as well as to the regulatory region.

Reduced levels of piRNAs in MILI- and MIWI2-deficient fetal testes

Although both *Mili* and *Miwi2* were expressed in fetal testes, the expression period of *Miwi2* was more re-

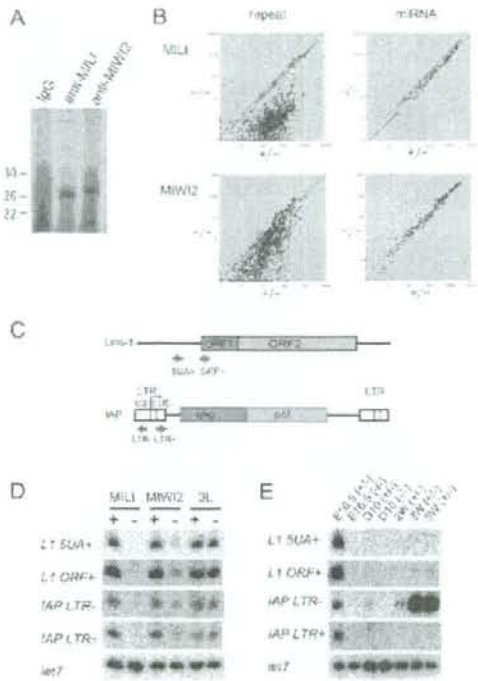

Figure 4. piRNA expression in MILI- and MIWI2-deficient fetal testes. (*A*) MILI- and MIWI2-bound piRNAs. The immunoprecipitated RNAs from E16.5 testicular lysates were ^{32}P-end-labeled and separated in a 15% denaturing urea–polyacrylamide gel. (*B*) Microarray analysis of the repeat-associated piRNAs and miRNAs. A microarray that contained 672 types of repeat-associated piRNAs and 150 types of miRNAs, both of which are expressed in fetal testes, was produced. RNA samples isolated from E16.5 control, MILI-deficient, and MIWI2-deficient mice were used. The expression of each small RNA was examined three times, and the mean values are plotted to compare the control and MILI- or MIWI2-deficient samples. Diagonal lines indicate a 1.5-fold difference in expression. (*C–E*) Expression of four arbitrarily selected piRNAs. piRNAs corresponding to the type A Line-1 promoter sense strand (5UA+), Line-1 ORF sense strand (ORF+), IAP LTR sense strand (LTR+), and IAP LTR antisense strand (LTR−) were arbitrarily selected. (*C*) The site and orientation of each piRNA is indicated by red arrows. (*D*) Northern blot analysis of the piRNAs in E16.5 control, MILI-deficient, MIWI2-deficient, and Dnmt3L-deficient testis. (*E*) Time-course analysis of the expression of the four piRNAs in control and MILI-null testes.

stricted (Supplemental Fig. S5) than that of *Mili* (Kuramochi-Miyagawa et al. 2001). *Miwi2* expression was reduced after birth, whereas *Mili* expression continued at essentially the same level throughout life. To examine the functions of MILI and MIWI2 in fetal testes, we determined whether the proteins bound to small RNAs. Ribonucleoprotein complexes from E16.5 testicular lysates were immunoprecipitated, the associated RNAs were isolated, and ^{32}P-labeling was carried out. As shown in Figure 4A, several RNAs of length 26–27 nt were coimmunoprecipitated with MILI and MIWI2.

Next, we used microarray analysis to test the roles of MILI and MIWI2 in the production of small RNAs in fetal testes. Using this method, we examined the expression patterns of 670 types of repeat-associated piRNAs and 150 types of miRNAs. As shown in Figure 4B, the vast majority of the piRNAs were significantly down-regulated in MILI-null fetal testes. Although this down-regulation was also observed in MIWI2-null testes, the mean fold reduction was smaller by one order of magnitude. In MILI-null fetal germ cells, ~88% of the piRNAs were present at less than one-eighth of the level in the control cells. In contrast, only 29% of the piRNAs in the MIWI2-null fetal germ cells were reduced to this level.

The relative levels of expression of the piRNAs that correspond to type Gf Line-1 and IAP are summarized in Table 1. In MILI-null testes, the expression levels of all of the type Gf Line-1 sense piRNAs and the vast majority of the type Gf Line-1 antisense piRNAs were less than one-quarter of the control. In contrast, the level of reduction was significantly lower in MIWI2-null testes. About 25% (27 of 101) and 14% (11 of 78) of the sense and antisense piRNAs, respectively, did not show significantly reduced expression in MIWI2-null testes. Notably, all of the piRNAs whose expression was unaffected by the MIWI2-null mutation were located in ORF1 and the endonuclease region of ORF2, whereas

Table 1. *Relative expression of the piRNAs for Line-1 Gf and IAP*

	Sense		Antisense	
Relative expression	MILI$^{-/-}$	MIWI2$^{-/-}$	MILI$^{-/-}$	MIWI2$^{-/-}$
(A) Line-1 Gf				
<1/64	63	0	44	3
1/64 ≤ <1/16	33	2	22	7
1/16 ≤ <1/4	5	23	10	26
1/4 ≤ <1/1.5	0	49	2	31
1/1.5 ≤ <1.5	0	22	0	10
1.5 ≤ <4	0	5	0	1
Total	101	101	78	78
(B) IAP				
<1/64	58	8	41	3
1/64 ≤ <1/16	42	7	10	3
1/16 ≤ <1/4	22	54	3	18
1/4 ≤ <1/1.5	1	43	0	22
1/1.5 ≤ <1.5	0	11	0	8
1.5 ≤ <4	0	0	0	0
Total	123	123	54	54

The relative expression levels of piRNAs that correspond to the type Gf Line-1 (A) and IAP (B) are shown. Relative expression is calculated from the microarray data and is shown as the ratio of the expression level of an individual piRNA in the MILI- and MIWI2-null mice to that in control mice. The numbers of piRNAs included in the relative expression range are described in the table.

none of these piRNAs were located in the reverse transcriptase region of ORF2. As with the type Gf Line-1 piRNAs, the expression levels of almost all of the piRNAs for IAP in the MILI-null testes were less than one-quarter of the control (Table 1), and the reduction was significantly less pronounced in the MIWI2-null testes. Unlike the case of Line-1, these piRNAs were not located in any special region.

We examined in greater detail the expression levels of four arbitrarily chosen piRNAs by Northern blot analysis using antisense oligonucleotides against small RNAs of 25–28 nt in length: the sense strand 5′-UTRs of type A (5UA+) and ORF (ORF+) for Line-1, and the sense and antisense strands of LTR (LTR+ and LTR−, respectively) for IAP (Fig. 3C). The sequences of LTR+ and LTR− were identical to those of the U3 region and R plus U5 region of LTR, respectively, and the expression levels of the four small RNAs were found to be quite similar in the E16.5 testes. As shown in Figure 4D, the four small RNAs were not detected in MILI-null testes, although they were weakly detected in MIWI2-null testes and expressed normally in Dnmt3L-null testes. The expression of the piRNAs was further examined in control and MILI-null testes during development, and 5UA+, ORF+, and LTR+ showed similar expression patterns (Fig. 4E). All three were expressed in fetal germ cells but were almost undetectable on day 10 and 2 wk after birth. Weak expression was detected 3 and 5 wk after birth. In contrast, the expression level of LTR− was higher 3 wk after birth than at E16.5.

Discussion

In the present study, we analyzed the mechanism of impaired retrotransposon silencing in MILI- and MIWI2-null male germ cells. DNA methylation of the regulatory regions of two retrotransposon species, Line-1 and IAP, was impaired from the stage of de novo methylation. Given that piRNAs are involved in gene silencing, we performed large-scale sequencing of the small RNAs in fetal male germ cells. Our data clearly indicate that the small RNA composition of fetal male germ cells is quite different from those of adult and neonatal prepachytene male germ cells. Finally, we compared the effects of MILI- and MIWI2-null mutations on the expression of repeat-associated piRNAs and found that these two mouse PIWI family proteins play similar but distinct roles in piRNA expression.

De novo DNA methylation and the murine PIWI proteins MILI and MIWI2

RT–PCR analysis showed that *Miwi2* expression commenced at E15.5 in male gonadal tissue (Supplemental Fig. S5). Meanwhile, *Mili* RNA was detected in male gonadal tissues beginning at E12.5. Therefore, both MILI and MIWI2 are expressed during de novo DNA methylation. Male germ cells from both MILI- and MIWI2-null mutant mice exhibited impaired DNA methylation in the regulatory regions of Line-1 and IAP soon after birth (Fig. 2A,B), which suggests that these two proteins play crucial roles in DNA methylation at an early stage of germ cell development. In addition, impaired de novo methylation was observed in MILI-deficient fetal germ cells. The significant reduction in piRNAs against the repeat-associated piRNAs in MILI- and MIWI2-deficient fetal testes implies that piRNAs are active in de novo DNA methylation.

Changes in piRNA content during male germ cell development

The compositions of the piRNAs and piRNA clusters were quite different during the process of male germ cell development; i.e., at the embryonic, neonatal prepachytene (Aravin et al. 2007), and adult stages (Aravin et al. 2006; Girard et al. 2006; Grivna et al. 2006; Lau et al. 2006; Watanabe et al. 2006). Although the fetal and neonatal piRNAs were similar in that each included a significant number of repeat-associated RNAs, they shared only 10% of the species in their piRNA clusters. Recently, it has been proposed that piRNA production involves a ping-pong amplification cycle for retrotransposon-related piRNAs (Brennecke et al. 2007; Gunawardane et al. 2007). The high proportion of piRNAs with U at the first nucleotide position and A at the tenth nucleotide position in our analysis of fetal repeats corresponding to piRNAs fits well with this hypothesis. However, the different compositions of the embryonic, neonatal, and adult piRNAs suggest that the cycle does not continue throughout male germ cell development, since the piRNAs in fetal germ cells are not maintained in adult germ cells (Fig. 4E). Therefore, some other mechanism(s) of piRNA biogenesis must operate during the pachytene phase to establish piRNA expression in adult germ cells.

We arbitrarily chose four fetal piRNAs and examined their expression in detail (Fig. 4E). All four piRNAs were either undetectable or weakly expressed in neonatal germ cells, although expression was somewhat increased after a couple of weeks. This also suggests that the molecular mechanism of piRNA production changes during development. At the same time, it implies that the function of piRNAs in embryos is different from that in neonates and adults.

MILI and MIWI2 have different functions

Impaired de novo methylation was detected in both MILI- and MIWI2-null male fetal germ cells. Although a general reduction in piRNA expression was observed in the mutants, the extent of the reduction was significantly different. As shown in Figure 4B, the reduction in numbers of piRNAs against repetitive sequences was much greater in the fetal germ cells of MILI-null testis than in those of MIWI2-null testis. This may reflect a difference in the molecular mechanisms of piRNA biogenesis between MILI and MIWI2.

The expression of several piRNAs was not reduced at all in MIWI2-null germ cells. In fact, 27 of 101 sense and 11 of 78 antisense Line-1 piRNAs were found to belong to this group (i.e., relative expression ≥1/1.5 in Table 1A). In contrast, the expression of these same piRNAs

was significantly reduced (i.e., relative expression <1/1.5 in Table 1A) in MILI-null germ cells. It is noteworthy that the vast majority of the piRNAs were located in ORF1 and the endonuclease region of ORF2 (Fig. 3C, ORF1 and Nu, respectively), although the significance of this result remains unclear. These data suggest that MILI and MIWI2 play different roles in the production, stabilization, and/or amplification cycle of piRNA.

Line-1 expression was similarly enhanced in MILI- and MIWI2-null testes (Fig. 1B), and bisulfite sequencing revealed that a significant reduction in DNA methylation occurred in both MILI- and MIWI2-null male germ cells (Fig. 2C). Considering that DNA methylation greatly influences retrotransposon transcription, the enhanced expression of Line-1 was correlated with DNA hypomethylation of the mutant male germ cells. The situation was a little different for IAPIΔ1 (Fig. 1B,D). Although defective DNA methylation was detected in both MILI- and MIWI2-null germ cells, IAPIΔ1expression was strongly increased in MILI-null testis, while it was either not increased or only slightly increased in MIWI2-null testis. These results imply different functions for MILI and MIWI2. Although it is difficult to explain the discrepancy, an as-yet-unknown post-transcriptional silencing mechanism may reduce IAP expression in MIWI2-null germ cells.

Molecular mechanisms of piRNA regulation

As described above, several aspects of piRNA regulation change significantly during development. For example, the piRNA composition differed among fetal, neonatal, and adult male germ cells. In addition, the first and tenth nucleotides and the distributions of piRNAs against the Line-1 or IAP sequence were different. Furthermore, although both MILI-null and MIWI2-null mice exhibited sterility owing to arrested spermatogenesis, the reductions in the percentages of piRNAs in their germ cells were significantly different. In addition, the regulatory mechanisms controlling IAPIΔ1 and Line-1 expression were different. It remains to be determined how the expression of IAPIΔ1, but not that of full-length IAP, is influenced by a null mutation of MILI or MIWI2. Finally, the mechanism of de novo methylation, presumably through piRNAs, remains an open question. Currently, it is difficult to propose a unified molecular mechanism to explain our results. Additional analyses will clarify the mechanisms underlying piRNA production and gene silencing.

Materials and methods

RNA extraction, RT–PCR, and Northern blot analysis

Total RNA samples were prepared from testes using Sepasol-RNA I Super (Nacalai Tesque), treated with DNase I, and subjected to RT–PCR with the ThermoScript RT–PCR System (Invitrogen) and random hexamers. Each reaction was performed using HotMaster Taq DNA polymerase and specific primers (Supplemental Table S6).

Northern blot analysis was performed at 65°C in 0.2 M $NaHPO_4$ (pH 7.2), 1 mM EDTA, 1% BSA, and 7% SDS. The membranes were washed with a 0.2× SSC/0.1% SDS solution at 65°C. The subcloned PCR products were labeled with [α-^{32}P]-dCTP and used as probes. The sequences used for PCR primers were as follows: the 3′-noncoding region of IAP (GenBank accession no. X04120), nucleotides 4489–4793; and the 5′-noncoding region of type Gf (D84391), nucleotides 874–1156, and A Line-1 (M13002), nucleotides 531–1642.

Methylation-sensitive Southern blot analysis

Whole-testis DNA was extracted from 2-d-old mice, and 3 µg of DNA were digested with KpnI and the methylation-sensitive restriction enzyme HpaII or the methylation-insensitive enzyme MspI. The type Gf Line-1 5′-noncoding region shown in Figure 1A was used as the probe.

Germ cell isolation

MILI mutant mice (Kuramochi-Miyagawa et al. 2004) and MIWI2 mutant mice were crossed with Oct-4/GFP transgenic mice (Yoshimizu et al. 1999) to obtain GFP-positive spermatogonia. Testis cells from embryos or pups were collected by two-step enzymatic digestion (Meistrich 1993), and the GFP-positive cells were sorted by FACS Aria (Becton Dickinson). Genomic DNA was extracted from the sorted germ cells.

Bisulfite methylation analysis

Bisulfite treatment of the genomic DNA isolated from fetal germ cells was performed using the EpiTect bisulfite kit (Qiagen). Two LTR regions of IAP (5.4-kb, IΔI-type) on chromosomes 3qD and 16qB2 were arbitrarily selected for analysis by nested PCR, and the products were sequenced. The first and second rounds of PCR were carried out using the primers F1 and R1, and F2 and R2, respectively. PCR amplification of the 5′-region of Line-1 (types Gf and A) was carried out using specific primers. The sequence of each primer is listed in Supplemental Table S6.

Anti-MILI and anti-MIWI2 antibodies

Affinity-purified anti-MILI-N2 (anti-mouse PIWIL2 [MILI], PM044; MBL Co., Ltd.) and anti-MIWI2-N1 polyclonal antibodies against MILI and MIWI2 were generated by immunization with peptides derived from MILI (amino acids 107–122: VRKDREEPRSSLPDPS) and MIWI2 (amino acids 31–45: TSASPGDSEAGGGTSC), respectively (MBL).

Small RNA cloning and sequencing

To isolate small RNAs, 20 µg of total RNA from E12.5–E19.5 male germ cells were gel-fractionated, and species 17–40 nt in length were gel-purified. The small RNAs were sequentially ligated to 3′- and 5′-adapters and then amplified by RT–PCR using a small RNA cloning kit (RR065; Takara Bio). Sequencing of the small RNA library was achieved using the 454 Life Science sequencer.

Annotation of the small RNAs

To identify the small RNAs that corresponded to various repeats (e.g., rRNA, tRNA, retrotransposon, and DNA transposon), the genomic positions of the repeats were retrieved from the University of California at Santa Cruz (UCSC) Web site (http://hgdownload.cse.ucsc.edu/downloads.html) and compared with the genomic positions of the small RNAs. When the genomic position of a particular small RNA overlapped with that of any repeat by up to 15 nt, the small RNA was considered to be repeat-derived. Repeat names were retrieved from all the

positions to which the small RNA mapped, and when multiple repeat names were retrieved, the class (e.g., LTR/MaLR and rRNA), and subclass (e.g., IAP), where applicable, were determined by the repeat with the greatest number of positions (Supplemental Table S2). When the top two repeats had the same number of positions, we did not determine the class or subclass. To identify small RNAs that corresponded to tRNAs, rRNAs, snRNAs, snoRNAs, scRNAs, miRNAs, piRNAs (known species from adult testes), and mRNAs based on sequence similarity, we extracted the sequences of the RNAs from GenBank (flat files, ftp://ftp.ncbi.nlm.nih.gov/genbank) and downloaded the remaining sequences from the following databases: for tRNAs, Genomic tRNA database (http://lowelab.ucsc.edu/GtRNAdb/Mmusc); for rRNAs, European ribosomal RNA database (http://www.psb.ugent.be/rRNA/index.html); for snoRNAs, snoRNA database (http://www-snorna.biotoul.fr) and RNA database (http://jsm-research.imb.uq.edu.au/rnadb); for piRNAs, RNA database (http://jsm-research.imb.uq.edu.au/rnadb); for miRNAs, miRBase (http://microrna.sanger.ac.uk/sequences/index.shtml); and for mRNAs, Refseq Genes (http://ftp.ncbi.nih.gov/refseq) and Ensemble Genes (http://www.ensembl.org/index.html). A BLAST search (http://ftp.ncbi.nih.gov/blast) was subsequently performed using our small RNA sequences as queries and our downloaded sequences as a database. Since sequence alignments using the BLAST program are local, a gap can hamper the alignment of short homologous sequences flanking the gap. Therefore, we extracted the sequences of the aligned regions from the data set with an extra 5 nt at both ends and realigned them with the small RNA sequences, using a global alignment program developed in-house that uses plural gap penalty parameter sets. We then classified the small RNAs using a 90% sequence identity threshold. Finally, the repeat annotations based on genomic position and the annotations based on sequence similarity were combined. For small RNAs with more than one annotation, we used the following order of priority: rRNA, tRNA, snoRNA, sc/srpRNA, miRNA, rasiRNA, piRNA, and mRNA. The unannotated sequences were classified as unknown.

Distribution and frequency of piRNAs corresponding to IAP and Line-1

The sequences of IAP1 (M17551) and L1_MdA (nucleotides 588–7713 of M13002) were retrieved from the flat files of GenBank. All of the small RNA sequences cloned were BLAST-searched against the IAP1 and L1_MdA sequences, using a cutoff *E*-value of 0.0001. The number of hits was determined every 100 nt.

Cluster analysis of small RNAs

We performed a cluster analysis of the male fetal gonadal small RNAs, with the following conditions: (1) The cluster should contain at least 11 types of small RNAs, and (2) the relative abundance of small RNAs between 24 and 28 nt in length should be greater than that of small RNAs between 19 and 23 nt in length.

Immunoprecipitation of the MILI ribonucleoprotein complex, and the isolation, labeling, and detection of small RNAs

E16.5 testes were homogenized in lysis buffer (20 mM HEPES at pH 7.5, 150 mM NaCl, 2.5 mM $MgCl_2$, 0.1% Nonidet P-40, 1 mM DTT) that contained protease inhibitors. Protein–RNA complexes were immunoprecipitated using anti-MILI-N2 and anti-MIWI2-N1 antibodies or normal rabbit serum as a control with Protein G Sepharose beads, and the RNAs were purified using ISOGEN-LS (Nippon Gene). The RNAs were labeled with [γ-^{32}P]-ATP using T4 polynucleotide kinase for 15 min at 37°C and then separated by 15% denaturing PAGE.

Microarray analysis

Total RNA from E16.5–E17.5 testes was purified using Sepasol-RNA I Super. For the rasiRNA probes, those sequences that were cloned more than six times and were >22 nt in length were selected from among the small RNAs that were annotated as repeats. In those cases where the small RNAs overlapped by 23 nt at their 5′-ends, a representative sequence was selected according to the number of clones. For the miRNA probes, we chose sequences that were cloned more than five times and were <23 nt in length from among the small RNAs that were annotated as miRNAs. In those cases where the small RNAs overlapped by 17 nt at their 5′-ends, a representative sequence was selected according to the number of clones. The target sequences for the microarray are listed in Supplemental Table S5. Microarray analysis was performed by a service provider (LC Sciences).

Small RNA Northern blotting

Northern blots were used to detect small RNAs, as described previously (Aravin et al. 2006), with 10 µg of total RNA loaded per well. The sequences of the probes used to detect the small RNAs are described in Supplemental Table S6. Hybridization was performed at 42°C in the same buffer used for regular Northern blotting. The membrane was washed twice with a 2× SSC/0.1% SDS solution at 42°C.

Acknowledgments

We thank Dr. Y. Matsui for providing the Oct-4/GFP mice, Dr. S. Tajima for providing the anti-Dnmt antibodies, and Ms. A. Kawai and Mr. K. Yoshinaga for assistance. We also thank Dr. K. Horie and Dr. Y. Kato for helpful discussions, and Ms. A. Mizokami for secretarial work. This work was supported in part by grants from the Japan Society for the Promotion of Science, the Ministry of Education, Culture, Sports, Science and Technology, the 21st Century COE Program "CICET," and the Uehara Memorial Foundation, Japan.

References

Aravin, A., Gaidatzis, D., Pfeffer, S., Lagos-Quintana, M., Landgraf, P., Iovino, N., Morris, P., Brownstein, M.J., Kuramochi-Miyagawa, S., Nakano, T., et al. 2006. A novel class of small RNAs bind to MILI protein in mouse testes. *Nature* **442:** 203–207.

Aravin, A.A., Sachidanandam, R., Girard, A., Fejes-Toth, K., and Hannon, G.J. 2007. Developmentally regulated piRNA clusters implicate MILI in transposon control. *Science* **316:** 744–747.

Bellve, A.R., Cavicchia, J.C., Millette, C.F., O'Brien, D.A., Bhatnagar, Y.M., and Dym, M. 1977. Spermatogenic cells of the prepuberal mouse. Isolation and morphological characterization. *J. Cell Biol.* **74:** 68–85.

Bourc'his, D. and Bestor, T.H. 2004. Meiotic catastrophe and retrotransposon reactivation in male germ cells lacking Dnmt3L. *Nature* **431:** 96–99.

Brennecke, J., Aravin, A.A., Stark, A., Dus, M., Kellis, M., Sachidanandam, R., and Hannon, G.J. 2007. Discrete small RNA-generating loci as master regulators of transposon activity in *Drosophila*. *Cell* **128:** 1089–1103.

Carmell, M.A., Girard, A., van de Kant, H.J., Bourc'his, D., Bestor, T.H., de Rooij, D.G., and Hannon, G.J. 2007. MIWI2 is

essential for spermatogenesis and repression of transposons in the mouse male germline. *Dev. Cell* **12:** 503–514.

Cox, D.N., Chao, A., Baker, J., Chang, L., Qiao, D., and Lin, H. 1998. A novel class of evolutionarily conserved genes defined by piwi are essential for stem cell self-renewal. *Genes & Dev.* **12:** 3715–3727.

Girard, A., Sachidanandam, R., Hannon, G.J., and Carmell, M.A. 2006. A germline-specific class of small RNAs binds mammalian Piwi proteins. *Nature* **442:** 199–202.

Grivna, S.T., Beyret, E., Wang, Z., and Lin, H. 2006. A novel class of small RNAs in mouse spermatogenic cells. *Genes & Dev.* **20:** 1709–1714.

Gunawardane, L.S., Saito, K., Nishida, K.M., Miyoshi, K., Kawamura, Y., Nagami, T., Siomi, H., and Siomi, M.C. 2007. A slicer-mediated mechanism for repeat-associated siRNA 5′ end formation in *Drosophila*. *Science* **315:** 1587–1590.

Hata, K., Kusumi, M., Yokomine, T., Li, E., and Sasaki, H. 2006. Meiotic and epigenetic aberrations in Dnmt3L-deficient male germ cells. *Mol. Reprod. Dev.* **73:** 116–122.

Houwing, S., Kamminga, L.M., Berezikov, E., Cronembold, D., Girard, A., van den Elst, H., Filippov, D.V., Blaser, H., Raz, E., Moens, C.B., et al. 2007. A role for Piwi and piRNAs in germ cell maintenance and transposon silencing in zebrafish. *Cell* **129:** 69–82.

Ishihara, H., Tanaka, I., Wan, H., Nojima, K., and Yoshida, K. 2004. Retrotransposition of limited deletion type of intracisternal A-particle elements in the myeloid leukemia CIIs of C3H/He mice. *J. Radiat. Res. (Tokyo)* **45:** 25–32.

Kalmykova, A.I., Klenov, M.S., and Gvozdev, V.A. 2005. Argonaute protein PIWI controls mobilization of retrotransposons in the *Drosophila* male germline. *Nucleic Acids Res.* **33:** 2052–2059.

Kato, Y., Kaneda, M., Hata, K., Kumaki, K., Hisano, M., Kohara, Y., Okano, M., Li, E., Nozaki, M., and Sasaki, H. 2007. Role of the Dnmt3 family in de novo methylation of imprinted and repetitive sequences during male germ cell development in the mouse. *Hum. Mol. Genet.* **16:** 2272–2280.

Kuramochi-Miyagawa, S., Kimura, T., Yomogida, K., Kuroiwa, A., Tadokoro, Y., Fujita, Y., Sato, M., Matsuda, Y., and Nakano, T. 2001. Two mouse piwi-related genes: miwi and mili. *Mech. Dev.* **108:** 121–133.

Kuramochi-Miyagawa, S., Kimura, T., Ijiri, T.W., Isobe, T., Asada, N., Fujita, Y., Ikawa, M., Iwai, N., Okabe, M., Deng, W., et al. 2004. Mili, a mammalian member of piwi family gene, is essential for spermatogenesis. *Development* **131:** 839–849.

Lander, E.S., Linton, L.M., Birren, B., Nusbaum, C., Zody, M.C., Baldwin, J., Devon, K., Dewar, K., Doyle, M., FitzHugh, W., et al. 2001. Initial sequencing and analysis of the human genome. *Nature* **409:** 860–921.

Lane, N., Dean, W., Erhardt, S., Hajkova, P., Surani, A., Walter, J., and Reik, W. 2003. Resistance of IAPs to methylation reprogramming may provide a mechanism for epigenetic inheritance in the mouse. *Genesis* **35:** 88–93.

Lau, N.C., Seto, A.G., Kim, J., Kuramochi-Miyagawa, S., Nakano, T., Bartel, D.P., and Kingston, R.E. 2006. Characterization of the piRNA complex from rat testes. *Science* **313:** 363–367.

Meistrich, M.L. 1993. *Cell and molecular biology of the testis*. Oxford University Press, New York.

Moussian, B., Schoof, H., Haecker, A., Jurgens, G., and Laux, T. 1998. Role of the ZWILLE gene in the regulation of central shoot meristem cell fate during *Arabidopsis* embryogenesis. *EMBO J.* **17:** 1799–1809.

Nolan, T., Braccini, L., Azzalin, G., De Toni, A., Macino, G., and Cogoni, C. 2005. The post-transcriptional gene silencing machinery functions independently of DNA methylation to repress a LINE1-like retrotransposon in *Neurospora crassa*. *Nucleic Acids Res.* **33:** 1564–1573.

Peters, L. and Meister, G. 2007. Argonaute proteins: Mediators of RNA silencing. *Mol. Cell* **26:** 611–623.

Reddien, P.W., Oviedo, N.J., Jennings, J.R., Jenkin, J.C., and Sanchez Alvarado, A. 2005. SMEDWI-2 is a PIWI-like protein that regulates planarian stem cells. *Science* **310:** 1327–1330.

Saito, K., Nishida, K.M., Mori, T., Kawamura, Y., Miyoshi, K., Nagami, T., Siomi, H., and Siomi, M.C. 2006. Specific association of Piwi with rasiRNAs derived from retrotransposon and heterochromatic regions in the *Drosophila* genome. *Genes & Dev.* **20:** 2214–2222.

Sakai, Y., Suetake, I., Shinozaki, F., Yamashina, S., and Tajima, S. 2004. Co-expression of de novo DNA methyltransferases Dnmt3a2 and Dnmt3L in gonocytes of mouse embryos. *Brain Res. Gene Expr. Patterns* **5:** 231–237.

Sarot, E., Payen-Groschene, G., Bucheton, A., and Pelisson, A. 2004. Evidence for a piwi-dependent RNA silencing of the gypsy endogenous retrovirus by the *Drosophila melanogaster* flamenco gene. *Genetics* **166:** 1313–1321.

Shi, H., Ullu, E., and Tschudi, C. 2004. Function of the Trypanosome Argonaute 1 protein in RNA interference requires the N-terminal RGG domain and arginine 735 in the Piwi domain. *J. Biol. Chem.* **279:** 49889–49893.

Tanaka, S.S., Toyooka, Y., Akasu, R., Katoh-Fukui, Y., Nakahara, Y., Suzuki, R., Yokoyama, M., and Noce, T. 2000. The mouse homolog of *Drosophila* Vasa is required for the development of male germ cells. *Genes & Dev.* **14:** 841–853.

Walsh, C.P., Chaillet, J.R., and Bestor, T.H. 1998. Transcription of IAP endogenous retroviruses is constrained by cytosine methylation. *Nat. Genet.* **20:** 116–117.

Watanabe, T., Takeda, A., Tsukiyama, T., Mise, K., Okuno, T., Sasaki, H., Minami, N., and Imai, H. 2006. Identification and characterization of two novel classes of small RNAs in the mouse germline: Retrotransposon-derived siRNAs in oocytes and germline small RNAs in testes. *Genes & Dev.* **20:** 1732–1743.

Webster, K.E., O'Bryan, M.K., Fletcher, S., Crewther, P.E., Aapola, U., Craig, J., Harrison, D.K., Aung, H., Phutikanit, N., Lyle, R., et al. 2005. Meiotic and epigenetic defects in Dnmt3L-knockout mouse spermatogenesis. *Proc. Natl. Acad. Sci.* **102:** 4068–4073.

Yoshimizu, T., Sugiyama, N., De Felice, M., Yeom, Y.I., Ohbo, K., Masuko, K., Obinata, M., Abe, K., Scholer, H.R., and Matsui, Y. 1999. Germline-specific expression of the Oct-4/green fluorescent protein (GFP) transgene in mice. *Dev. Growth Differ.* **41:** 675–684.

Zaratiegui, M., Irvine, D.V., and Martienssen, R.A. 2007. Noncoding RNAs and gene silencing. *Cell* **128:** 763–776.

19

Sperm–Egg Fusion Assay in Mammals

Naokazu Inoue and Masaru Okabe

Summary

As representatives of the 60 trillion cells that make a human body, a sperm and an egg meet, recognize each other, and fuse to create a new generation. Thus, gamete fusion is an extremely important process that must transpire without error to launch life activity. This may drive the fusion mechanism to evolve into an unfailing and steady process. At the same time, fusion must be restricted to occur only between two gametes of the same species. However, the molecular bases of the fusion event in fertilization have not yet been clarified. In this chapter, we describe the methods to evaluate fusion by staining the swollen sperm nuclei after fertilization.

Key Words: Sperm; egg; fusion; fertilization; Izumo.

1. Introduction

Fertilization is well known as one of the most typical cell–cell fusion processes in vivo. Among the many ejaculated sperm journeying into the uterus, and subsequently to the ampulla of the oviduct, only a few bump into eggs. At the final stage of the long journey, a selected sperm penetrates into the zona pellucida (ZP) that surrounds the eggs and fuses with the egg plasma membrane. Until recently, the molecular basis for fertilization was poorly understood, especially the final sperm–egg fusion process.

To identify factors involved in sperm–egg fusion, we utilized an antimouse sperm monoclonal antibody OBF13 that specifically inhibits the fusion process, and we succeeded in finding a novel fusion factor that we named *Izumo* after the Japanese shrine dedicated to marriage *(1)*. On the egg plasma membrane, the fusion-related protein CD9 was discovered rather serendipitously by three groups *(2–4)*. In those studies, the assessment of fusion was performed by either the Hoechst prestain or poststain method described below. At present, Izumo and CD9 are the only factors that have been proved to be indispensable

From: *Methods in Molecular Biology, vol. 475: Cell Fusion: Overviews and Methods*
Edited by: E. H. Chen © Humana Press, Totowa, NJ

through gene-manipulated animals. Elucidation of the real central factor of the fusion machinery is yet to come.

2. Materials

2.1. Preparation of Oocytes

1. Female mouse 8 weeks old (or older) of an appropriate strain (10 weeks old or older female if hamster).
2. Hypodermic needle, 30 gauge, 1/2 inch syringe, 1 mL sterile disposable.
3. Pregnant mare's serum gonadotropin (PMSG; Sigma, St. Louis, MO, catalog number G-4877), human chorionic gonadotropin (hCG; Sigma, catalog number C-1063) for superovulation.
4. Hyaluronidase type IV-S (Sigma, catalog number H-4272).
5. 30- or 60-mm no surface coated plastic dish for bacteria (Iwaki, Holliston, MA, numbers 1000-035, 1010-060).
6. Watchmaker's forceps (Fontax 5C).
7. Egg-handling pipette (finely drawn capillary tube (Funakoshi 1-40-7500) with mouth pipette (Sigma, catalog number A5177).
8. Stereoscopic microscope (Olympus SZX12).
9. CO_2 incubator (37 °C, 5%CO_2, Asshi 4020).
10. Modified kSOM medium (for culture of mouse eggs; **Table 1**).
11. FHM medium (for collection of mouse eggs; *see* **Table 1**).
12. BWW medium (for culture of hamster eggs; *see* **Table 1**), modified BWW medium (containing 3 mg/mL of human serum albumin [HAS: Sigma catalog number A-1653]).
13. Mineral oil (Sigma, catalog number M-8410).

2.2. Removal of the Zona Pellucida

1. Piezo-manipulator PMAS-CT150 (Prime Tech LTD, Japan).
2. Stereoscopic microscope.
3. Egg-handling pipette.
4. Acidic Tyrode's solution (Sigma, catalog number T-1788).
5. Borosilicate glass tube (Sutter Instrument Co., Novato, CA, B100-75-10).
6. Sutter P97 puller to make a 10-μm diameter capillary.
7. 12.5% PVP in Hepes-CZB (*see* **Table 1**).
8. Mineral oil.

2.3. Collection of Sperm

1. 10-week-old (or older) appropriate strain male mouse.
2. Human sperm from healthy male donors.
3. TYH medium (for capacitation of mouse sperm; *see* **Table 1**).
4. Modified BWW medium (for capacitation of human sperm; *see* **Table 1**).
5. Watchmaker's forceps (Fontax 5C).

Table 1
Composition of Media

Reagent	Source	Modified kSOM	FHM	TYH	BWW	Hepes-CZB
NaCl	Sigma S-5886	2.775 g	2.775 g	3.488 g	2.455 g	2.38 g
KCl	Sigma P-5405	0.093 g	0.093 g	0.178 g	0.178 g	0.18 g
KH_2PO_4	Sigma P-5655	0.0238 g	0.0238 g	0.081 g	0.081 g	0.08 g
$MgSO_4$	Sigma M-2643	0.012 g	0.012 g	0.072 g	0.072 g	0.071 g
Sodium lactate (60% [w/v])	Sigma L-7900	1.18 mL	1.18 mL	—	1.54 mL	1.85 mL
Sodium pyruvate	Sigma P-4562	0.011 g	0.011 g	0.028 g	0.014 g	0.0176 g
Glucose	Sigma G-6152	0.018 g	0.018 g	0.5 g	0.5 g	0.5 g
Glutamine (200 m*M* stock)	Sigma G-7513	2.5 mL	2.5 mL	—	—	2.5 mL
Bovine serum albumin	Sigma A-3311	0.5 g	0.5 g	2.0 g	—	1.5 g
EDTA 0.2 Na	Sigma E-6635	—	—	—	—	0.0205 g
EDTA 0.4 Na (10 m*M*	Dai-ichi 1.3 mL × 10	0.5 mL	0.5 mL	—	—	—
$NaHCO_3$	Sigma S-5761	1.05 g	0.168 g	1.053 g	1.5 g	0.21 g
Hepes	Sigma H-6147	—	2.38 g	—	—	2.6 g
$CaCl_2/2H_2O$	Sigma C-7902	0.126 g	0.126 g	0.126 g	0.126 g	0.125 g
Essential amino acid	GibcoBRL 11130-051	10 mL	10 mL	—	—	—
Nonessential amino acid	GibcoBRL 11140-050	5 mL	5 mL	—	—	—
Penicillin-streptomycin	GibcoBRL 15140-148	2.5 mL	2.5 mL	2.5 mL	2.5 mL	2.5 mL
Phenol Red 0.5%	Dai-ichi 1.3 mL × 10	1.0 mL	1.0 mL	0.5 mL	0.5 mL	1.0 mL
1.0 N NaOH	Nacalai tesque 315-11	—	Adjust to pH 7.4	—	—	Adjust to pH 7.4
Water	GibcoBRL 15230-162	Adjust to 500 mL	Adjust to 500 mL	Adjust to 500 mL	Adjust to 500 mL	Adjust to 500 mL

These medium were filtrated with 0.2 μm filter, divided into 10 mL, and stored at –20°C until used.

6. Straight-blade Vannas scissors (Natume MB54-1).
7. Stereoscopic microscope.
8. CO_2 incubator.
9. 30- or 60-mm nontreated plastic dish.
10. Mineral oil.

2.4. Staining of Fused Sperm

1. Hoechst 33342 (Invitrogen H-3570).
2. CO_2 incubator.
3. 0.25% glutaraldehyde for fixation.
4. Stereoscopic microscope.
5. Ix-70 fluorescent microscope (Olympus).
6. Egg-handling pipette.
7. Mineral oil.
8. Mixture of solid paraffin and Vaseline (mixing ratio is 1:9).

3. Methods

3.1. Preparation of Oocytes

This procedure is described in more detail by Nagy et al. *(5)*.

1. Intraperitoneal injections of 5 IU PMSG and 5 IU hCG at a 48-h interval to 8-week-old (or older) female mice (injection 30 IU PMSG and 30 IU hCG at 72-h interval to 10-week-old or older female hamster).
2. Sacrifice the mice at 13–15 h after hCG injection (sacrifice the hamster at 17 h after hCG).
3. Dissect the oviducts.
4. Transfer the oviduct to a mineral oil–covered 30- or 60- mm plastic dish.
5. Newly ovulated oocytes, surrounded by cumulus cells, are found in the ampulla of oviduct.
6. Place one oviduct beside a mineral oil–covered 100-μL drop of FHM medium prepared on 60-mm plastic dish.
7. Use watchmaker's forceps to grasp the oviduct and supplementary forceps to tear the oviduct close to where the oocytes are located.
8. Release the clutch of cumulus cells into a 100 μL drop of FHM medium.
9. Allow eggs to incubate in 35 IU/mL hyaluronidase solution until the cumulus cells are completely removed (it may take approximately 5 min).
10. Wash eggs by pipetting in and out and subsequently transferring eggs into fresh drops of FHM medium (repeat at least three times).
11. Place up to 50 eggs in a 50-μL drop of modified kSOM at 37 °C under 5% CO_2 in air until removal of the zona pellucida is performed.

3.2. Removal of the Zona Pellucida

Two different methods for the preparation of zona pellucida–free eggs are described. Acidic Tyrode's method is a quick and easy method to remove zona

pellucida and is often used by researchers. However, a drawback of this method is that a part of the dissolved zona pellucida was found to be readsorbed on the egg plasma membrane *(6)*. In natural conditions, the acrosome intact sperm do not bind to egg plasma membrane, but with acidic Tyrode's method we cannot eliminate a massive adhesion between acrosome intact sperm and eggs with readsorbed zona pellucida on their plasma membrane. Because this "false binding" can be eliminated by mechanical zona pellucida removal methods as shown in **Figures 1** and **2** *(6)*, we always use this method to perform sperm–egg fusion assay. The other available mechanical removal method is reported by another group *(7)*.

3.2.1. Acidic Tyrode's Method

1. Prepare eggs and remove cumulus cells as described in **Subheading 3.1.**
2. Transfer cumulus-free eggs into a 50-µL drop of mineral oil–covered acidic Tyrode's solution prepared on a plastic dish.
3. To remove remnant medium, transfer eggs into a second 50 µL of acidic Tyrode's solution.
4. Repeatedly pipette the eggs in and out until the zona pellucida are dissolved under the stereoscopic microscope (it may be finished within 30 s).
5. Wash zona pellucida–free eggs at least three times by transferring eggs into fresh new drops of TYH medium to remove remnant acidic Tyrode's solution. (For human sperm, modified BWW medium is required instead of TYH medium.)

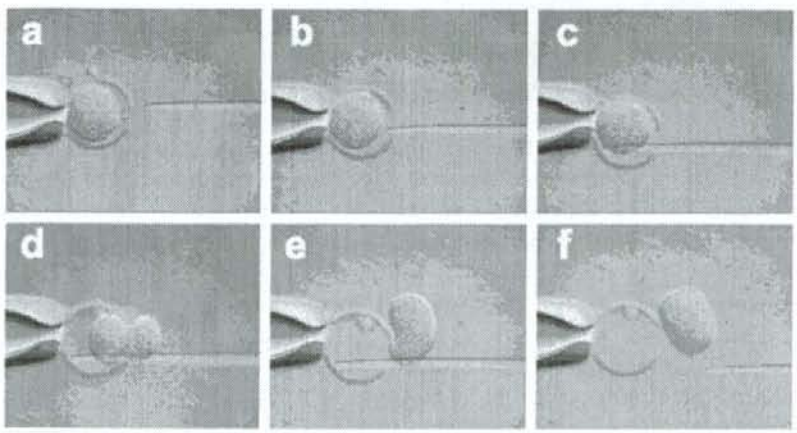

Fig. 1. Preparation of zona pellucida–free eggs using a piezo-micromanipulator. Eggs were freed from the cumulus cells and placed in a drop of FHM. A pipette, attached to a piezo-driven micromanipulator, was used to form a slit in the zona pellucida (**A,B**). The egg then was flushed out through the slit by rapidly introducing medium into the perivitelline space from behind the eggs (**C–F**).

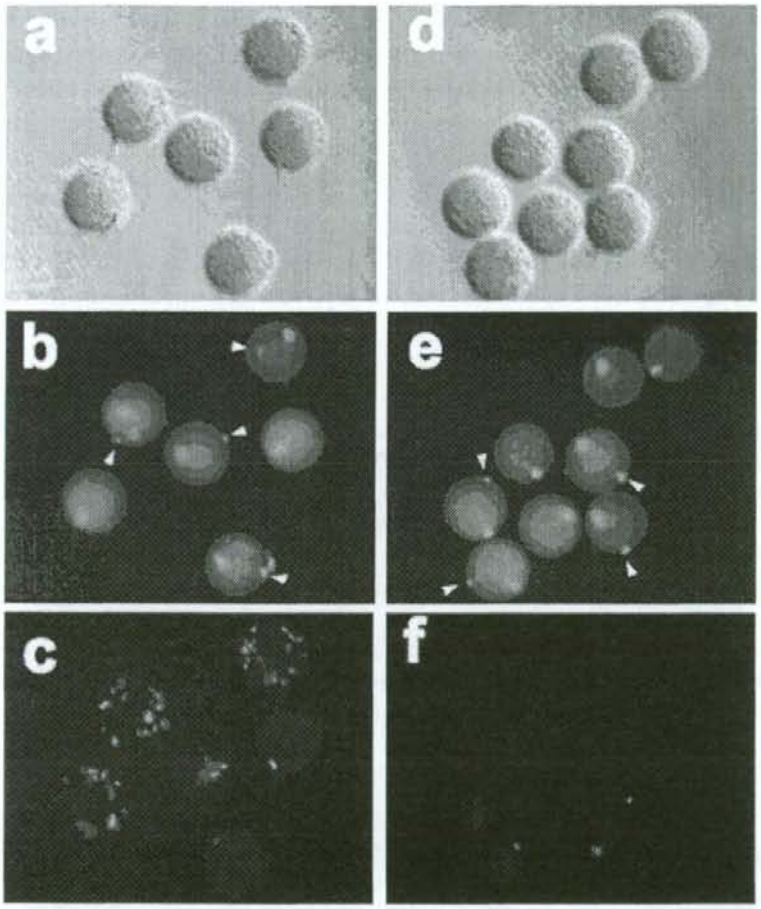

Fig. 2. An example of the Hoechst "preloading" method: comparison of sperm binding and fusing abilities to denuded egg plasma membrane (PM) by acidic Tyrode's (acid PM) or manipulator (piezo PM). "Green sperm" from *Acr-EGFP* transgenic mice *(8)* were capacitated for 2 h and then mixed with eggs preloaded with Hoechst 33342 that were prepared with acidic Tyrode's solution (in A–C) and a piezo-manipulator (in D–F). After 30 min of incubation, eggs were fixed and visualized by fluorescence microscopy to assay sperm PM binding and fusion. **(A,D)** Bound sperm (Hoffman modulation contrast optics). Considerably more sperm were present on the acid PM than on the piezo PM. **(B,E)** Fused sperm are stained with Hoechst (arrowheads) because of the dye transfer from the egg. Similar numbers of fused sperm were seen with both types of egg preparation. The larger egg nucleus was also stained. **(C,F)** Acrosome intact sperm had "green fluorescent" acrosomes. The majority of sperm bound to eggs prepared with the acidic Tyrode's solution were acrosome intact, while few sperm prepared by the piezo-micromanipulator that bound to eggs were acrosome intact.

6. Incubate in TYH medium for more than 1 h at 37 °C under 5% CO_2 in air to allow surface proteins to recover.

3.2.2. Mechanical Method Using a Piezo-Manipulator

1. Prepare eggs and remove cumulus cells as described in **Subheading 3.1** (**see Fig. 1; ref. *6***).
2. Prepare the drilling pipette from a borosilicate glass tube by pulling using a Sutter P97 puller to a diameter of 10 µm according to an appropriate textbook (***5***).
3. Add a few microliters of mercury to the tip of the pipette to enhance the drilling efficiency.
4. Prepare several 6-µL drops of mineral oil–covered 12.5% PVP in Hepes-CZB and FHM media prepared on the top of a 60-mm plastic dish.
5. Equip the pipette to the piezo-driven micromanipulator and first soak the pipette wall with 12.5% PVP in Hepes-CZB.
6. Make an approximately 30-µm slit in the zona pellucida by applying a piezo-pulse (*see* **Fig. 1**).
7. Flush out the oocyte from the slit by rapidly introducing medium into the perivitelline space from behind the eggs (*see* **Fig. 1**).
8. Place up to 50 zona pellucida–free eggs into a 50 µL drop of TYH medium and incubate at 37 °C under 5% CO_2 in air until use.

3.3. Collection of Sperm

3.3.1. Human Sperm

1. Collect sperm from healthy male donors by masturbation.
2. Liquefy for 30–60 min at 37 °C under 5% CO_2 in air and divide into 0.5-mL aliquots.
3. Place 0.5-mL aliquots to the bottom of 2 mL of modified BWW medium.
4. Incline the tubes to an angle of 30 ° and incubate at 37 °C under 5% CO_2 in air for 1 hr.
5. Take out approximately 1.0 mL of the upper part of the medium containing motile sperm into another 1.5-mL tube.
6. Centrifuge for 5 min at 500 *g* at room temperature.
7. Discard supernatant and resuspend the sperm in 1 mL of modified BWW medium.
8. Repeat **steps 6** and **7** twice more. Eventually resuspend in a mineral oil–covered 400-µL drop of modified BWW medium prepared on 60-mm plastic dish at 37 °C under 5% CO_2 in air until use.

3.3.2. Mouse Sperm

1. Dissect the cauda epididymis from 12-week-old (or older) mice according to textbook (***5***).
2. Place the epididymis beside a 100-µL drop of TYH medium covered by mineral oil in a 30- or 60-mm plastic dish.

3. Use watchmaker's forceps to grasp the cauda epididymis and make a cut at the proximal cauda epididymis (mature sperm are stored) with straight-blade Vannas scissors.
4. After squeezing the sperm out from the cut area, hold the swarm of sperm by sticking them to the tip of supplementary forceps.
5. Introduce the swarm of sperm into a 200-μL drop of TYH medium.
6. At 1 h after incubation, check the sperm motility by observing well-dispersed sperm.
7. Cultivate sperm for an additional 1 h in TYH medium at 37 °C under 5% CO_2 in air to induce capacitation and spontaneous acrosome reaction before insemination.

3.4. Staining of Fused Sperm

Fusion assessment can be performed in two different ways.

3.4.1. Hoechst "Preloading" Method

1. Prepare the zona pellucida–free eggs as described in **Subheading 3.2**.
2. Introduce eggs into a 50-μL drop of Hoechst 33342 (1 μg/mL) in TYH medium (up to 50 eggs per spot), and allow to stand for 10 min at 37 °C under 5% CO_2 in air.
3. Transfer the eggs into another fresh 50-μL drop of TYH medium covered with mineral oil.
4. Incubate dye-loaded eggs for 15 min at 37 °C under 5% CO_2 in air to discharge excess dye.
5. Repeat **steps 3** and **4** three more times, and subject to fusion assay.
6. Cultivate sperm as described in **Subheading 3.3**. to induce capacitation.
7. Transfer the eggs into a 50-μL drop of FHM medium containing 0.25% glutaraldehyde for fixation after 30 min of incubation with 2×10^5 mouse sperm.
8. Allow to stand for 5 min at room temperature.
9. Wash the sperm-bound eggs by transferring eggs into fresh drops of FHM medium several times
10. Observe under a fluorescence microscope (ultraviolet excitation light). With this method, only nuclei of fused sperm are stained by the dye transferred into sperm after membrane fusion (*see* **Fig. 2** and **3**; **Note 1**).

3.4.2. Hoechst "Poststaining" Method: Observation of Swollen Sperm

1. Prepare the zona pellucida–free eggs as described in **Subheading 3.2.**
2. Cultivate sperm as described in **Subheading 3.3.** to induce capacitation.
3. Prepare a 100-μL drop of TYH medium covered by mineral oil prepared on 60-mm plastic dish.
4. Introduce zona pellucida–free eggs into a drop of TYH medium.
5. Incubate zona pellucida–free eggs with 2×10^5 (for mouse) or 1×10^6 (for human) sperm for 6 h in TYH or modified BWW medium at 37 °C under 5% CO_2 in air,

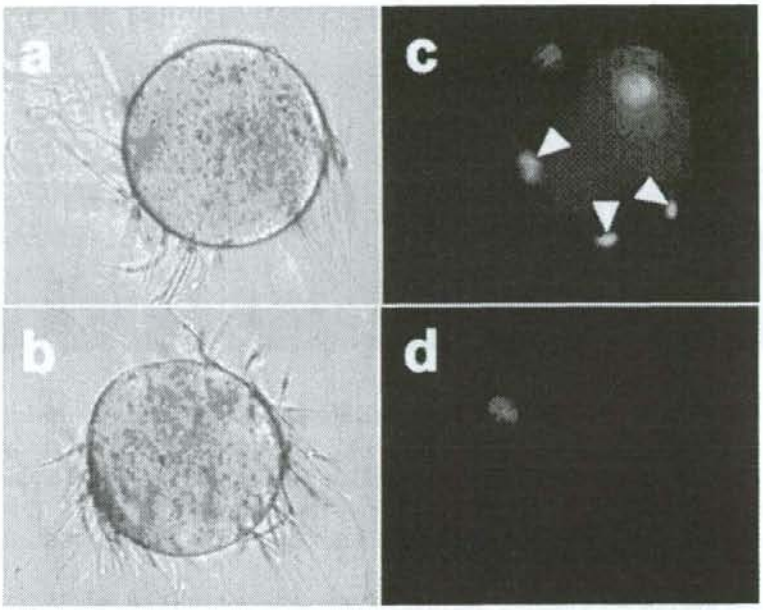

Fig. 3. An example of the Hoechst "preload" method: fusion assay of Izumo knockout sperm. Fused sperm were stained by the egg that was preloaded with Hoechst 33342. The arrowheads show the fused sperm. In comparison with a few *Izumo* +/– sperm, which successfully fused with eggs **(A,C)**, *Izumo* –/– sperm never fused with eggs **(B,D).** This defect was limited to the fusion process, because pups from *Izumo* –/– sperm could be obtained by intracytoplasmic sperm injection. (Reprinted from **ref. *1*** with permission of Nature Publishing Group.)

respectively. Fused sperm heads launch to swell during this incubation period; some enlarged sperm heads can be seen under a phase contrast microscope.

6. Wash the sperm bound eggs by pipetting and transferring into fresh new drops to remove weakly bound sperm.
7. Incubate the eggs with 1 μg/mL of Hoechst 33342 for 10 min at 37 °C under 5% CO_2 to stain swollen sperm nucleus.
8. Wash the eggs several times by transferring them into fresh TYH medium.
9. To observe sperm-fused eggs, apply four small dabs of Vaseline mix (vaseline: solid paraffin = 9:1) on a slide glass by injecting out from a syringe without needle.
10. Place a few eggs into a 1-μL drop of FHM medium, and cover the eggs with a cover glass.
11. Gently press the eggs with the cover glass to flatten the eggs under the stereoscopic microscope to make the observation easier (*see* **Note 2**).
12. Observe under a fluorescence microscope (ultraviolet excitation light).

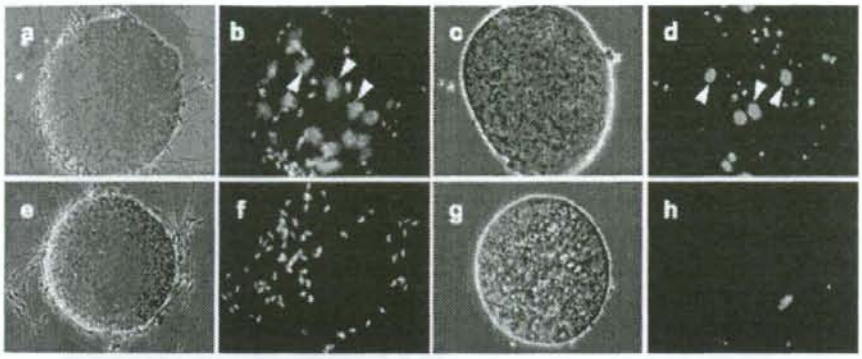

Fig. 4. Exemplification of Hoechst "poststain" method: involvement of Izumo in the xeno-species fusion system. Six hours after the insemination of zona pellucida–free hamster eggs with *Izumo* +/– **(A,B)** and –/– **(E,F)** mouse sperm, sperm heads were stained by adding Hoechst 33342 to the medium **(B,F)**. The sperm–egg binding was strong enough to resist the repeated pipetting. Human sperm were also added with 25 µg/mL of antihuman Izumo **(G,H)** or control IgG **(C,D)** to zona pellucida–free hamster eggs. No fusion was observed in the presence of anti-Izumo antibody. The arrowheads indicate the swelling sperm head after staining with Hoechst 33342 **(B,D)**. (Reprinted from **ref.** *1* with permission of Nature Publishing Group.)

Fused sperm (enlarged heads) will be stained with the dye as in **Figure 4**. (For human sperm, the use of modified BWW medium is required instead of TYH medium; *see* **Note 3.**)

4. Notes

1. The Hoechst "preloading" method is not applicable when hamster eggs are used. They seem to pump out the Hoechst dye from the cytosol. As a result, hamster eggs are not able to accumulate enough dye for fusion assay (*see* **Subheading 3.4.1.**).
2. For the observation of swollen sperm, the cover glass is pressed down to squeeze the eggs such that the sperm become more visible, but this has to be done carefully. The eggs burst easily with excess amount of pressurization (*see* **Subheading 3.4.2.**).
3. The mixing of gametes of xeno species is ethically restricted in many ways. Please follow the ethical laws in the countries where the experiments are pursued (*see* **Subheading 3.4.2.**).

References

1. Inoue, N., Ikawa, M., Isotani, A., and Okabe M. (2005) The immunoglobulin superfamily protein Izumo is required for sperm to fuse with eggs. *Nature* **434,** 234–238.
2. Le Naour, F., Rubinstein, E., Jasmin, C., Prenant, M., and Boucheix, C. (2000) Severely reduced female fertility in CD9-deficient mice. *Science* **287,** 329–321.

3. Miyado, K., Yamada, G., Yamada, S., Hasuwa, H., Nakamura, Y., Ryu, F., Suzuki, K., Kosai, K., Inoue, K., Ogura, A., Okabe, M., and Mekada, E. (2000) Requirement of CD9 on the egg plasma membrane for fertilization. *Science* **287,** 321–324.
4. Kaji, K., Oda, S., Shikano, T., Ohnuki, T., Uematsu, T., Sakagami, J., Tada, N., Miyazaki, S., and Kudo, A. (2000) The gamete fusion process is defective in eggs of Cd9-deficient mice. *Nat. Genet.* **24,** 279–282.
5. Nagy, A., Gertsenstein, M., Vintersten, K., and Behringer, R. (2002) *Manipulating the Mouse Embryo*, 3rd ed. Cold Spring Harbor Laboratory Press, Cold Spring Harbor, NY.
6. Yamagata, K., Nakanishi, T., Ikawa, M., Yamaguchi, R., Moss, S, B., and Okabe, M. (2002) Sperm from the calmegin-deficient mouse have normal abilities for binding and fusion to the egg plasma membrane. *Dev. Biol.* **250,** 348–357.
7. Ziyyat, A., Rubinstein, E., Monier-Gavelle, F., Barraud, V., Kulski, O., Prenant, M., Boucheix, C., Bomsel, M., and Wolf, J. P. (2006) CD9 controls the formation of clusters that contain tetraspanins and the integrin alpha 6 beta 1, which are involved in human and mouse gamete fusion. *J. Cell Sci.* **119,** 416–424.
8. Nakanishi, T., Ikawa, M., Yamada, S., Parvinen, M., Baba, T., Nishimune, Y., and Okabe, M. (1999) Real-time observation of acrosomal dispersal from mouse sperm using GFP as a marker protein. *FEBS Lett.* **449,** 277–283.

特集　月経困難症に対する治療戦略

子宮腺筋症の疼痛対策

浅田弘法[*1]　羽田智則[*1]　梶谷宇[*1]
内田浩[*1]　浜谷敏生[*1]　丸山哲夫[*1]
吉村泰典[*1]　岸郁子[*2]　木挽貢慈[*3]

はじめに

子宮腺筋症は，子宮筋層に子宮内膜症病巣が侵入，あるいは発生したものである．子宮腺筋症の発症率は報告によって大きく異なり，数%というものから40～70％という報告まである[1,2]．このような発症率の違いは，診断基準や，摘出子宮の検索方法の相違によって生じると考えられる．また，これらの摘出子宮による評価ではもともと検索した子宮が疾患を伴った子宮であるため，検討した集団に偏りがあり，いわゆる発症率・有病率は明確にはなっていないのが現状である．

一方，臨床的には病理学的な診断とは別に臨床症状と画像診断により子宮腺筋症を診断している．画像診断として，経腟超音波およびMRIが普及してきたため，診断率は向上してきた．特にMRIによる診断は強磁場のMRIが普及してきたこともあり，きわめて重要な情報を提供してくれる．子宮腺筋症の臨床症状としては月経困難症と過多月経が主たる症状であるが，過多月経の症状は40～50％に，月経困難症の症状は約15～30％の子宮腺筋症患者に認められると報告されている[1]．超音波診断およびMRIで診断した場合，子宮腺筋症診断のsensitivityおよびspecificityは約80～90％と報告されている[3]．

従来は画像診断による子宮腺筋症の診断が困難であったため，子宮腺筋症と妊孕能，子宮腺筋症と切迫流早産および子宮破裂などの妊娠合併症，子宮腺筋症と子宮体癌などの関連性についてはprospectiveに評価することはできなかった．そのため，現状では診療のよりどころになるようなデーターはない．一方，子宮内膜症と月経困難症との関連性は多数の報告が存在している．子宮腺筋症は，深部子宮内膜症の一亜型であると考えることができるので，ダグラス窩子宮内膜症，直腸子宮内膜症などのいわゆる深部内膜症と称される，硬結を伴う子宮内膜症に対する治療法と同様の治療方法が子宮腺筋症に対しても有効であると推測される．硬結を伴う深部子宮内膜症病変の治療は，薬剤の効果が少ないことから，切除が基本的な治療である．子宮腺筋症によって発症する疼

Asada Hironori
*1 慶應義塾大学医学部産婦人科学教室
（〒160-8582 東京都新宿区信濃町35番地）
*2 東京歯科大学市川総合病院産婦人科
*3 川崎市立川崎病院産婦人科